Ozone Generation in Dry Air Using Pulsed Discharges With and Without a Solid Dielectric Layer

W. J. M. Samaranayake, Y. Miyahara, T. Namihira, S. Katsuki, R. Hackam[1] and H. Akiyama

Department of Electrical and Computer Engineering
Kumamoto University
Kumamoto, Japan

ABSTRACT

Energy efficient generation of ozone is very important because ozone is being used increasingly in a wide range of industrial applications. Ozonizers usually use dielectric barrier discharges and employ alternating current (ac) with consequent heat generation, which necessitates cooling. In the present study, very short duration pulsed voltage is employed resulting in reduced heating of the gas and discharge reactor. A comparison of ozone generation in dry air using a coaxial concentric electrode system with and without a solid dielectric layer is reported. Two types of dielectric layers were employed, ceramic and polyvinylchloride (PVC). The effects of peak pulsed voltage (12.5 to 62 kV), reactor length (0.1 to 1 m), pulse repetition rate (25 to 400 pulses per second, pps), gas flow rate (1.5 to 3.0 l/min) and variation of the pitch length of the spiral wire forming the central electrode (5 to 10 mm) on the concentration and production yield of ozone (g/kWh) are reported. A comparison is made between the performance of discharge reactors with (ceramic reactor Type IIC and PVC reactor Type IIP) and without (reactor Type I) a dielectric layer, using the same electrode gap separation (15 mm) and reactor lengths (0.157 and 1 m). High production yields of ozone in dry air of $\sim$ 122, 52 and 60 g/kWh were obtained when using, respectively ceramic, PVC, and no dielectric layer, for a fixed pulse rate of 100 pps, 1.5 l/min flow rate and for a relatively short length of the reactor of 157 mm.

1 INTRODUCTION

THE generation of ozone using a solid dielectric barrier placed adjacent to the cathode in a concentric coaxial electrode system is an important application of non-thermal discharges for gaseous plasma synthesis. The generation of ozone using air instead of oxygen is advantageous due to the readily available air, which obviates the requirement of cryogenic systems for producing oxygen. Ozone has numerous applications as a potent germicide and viricide, as well as a strong bleaching agent, and is increasingly used to replace other oxidants [1–4]. Conventional oxidizing agents may cause hazards during storage, handling and transportation and therefore, ozone represents a good choice to prevent these disadvantages. This is because ozone can neither be stored nor shipped due to its inherent instability [1] and therefore, it is usually generated on the site where it is used. HV short-pulse power has been shown to be very effective in applications for plasma synthesis [5]. The main merits of using short-pulse power are that the temperature of the ions and of the neutral gas does not increase much above the ambient during the short duration of the pulse [6], and breakdown leading to an arc and collapse of the gap voltage does not readily occur [7–12]. The high-energy electrons in the streamers dissociate the oxygen molecules present in the air into atoms and these collide with an oxygen molecule and a third particle to produce ozone [2, 13].

The use of very short HV pulses combined with a dielectric layer placed adjacent to the cathode results in a short lifetime of the streamers. This results in less energy transferred into the ions and the neutral gas, which obviates the need to use elaborate cooling system to remove the heat from the electrodes, with the consequent increase in the energy cost of generating the ozone. The presence of the dielectric layer mitigates against the development of an arc discharge and thus promotes the development of streamer discharges [14]. The dielectric layer also reduces electron emission from the cathode, which further inhibits the streamer-arc transition [1]. The dielectric layer reduces the charge transported by a single streamer and distributes the streamers over a wide area near the dielectric layer [1].

In the present study, the concentration of ozone and the production yield in g/kWh were determined in a coaxial electrode configuration employing ceramic and PVC layers, and were compared also with the

1070–9878/1/ $3.00 © 2001 IEEE

concentration and the production yield of ozone using a reactor without a dielectric barrier. The effects on the production of ozone of a wide range of parameters including voltage level, reactor length, pulse repetition rate, gas flow rate and variation of the pitch length of the spiral wire forming the central electrode, were investigated. Throughout this work the measurements were performed in a regime before the streamers transferred into an arc.

2 EXPERIMENTAL TECHNIQUES AND PROCEDURE

2.1 EXPERIMENTAL TECHNIQUES

Figure 1 shows a schematic diagram of the experimental setup to generate ozone. Dry air was obtained from a gas cylinder which had concentrations of nitrogen 78.08%, oxygen 20.95%, carbon dioxide 0.03%, argon 0.93% and traces of neon, helium, methane, krypton, xenon, hydrogen and nitrous oxide [15]. The air was fed axially into the reactor using two flow rates of 1.5 and 3.0 l/min. The flow rate was measured using a flow-stat meter. The concentration of ozone was measured using an ultraviolet (UV) absorption meter at 253.7 nm, which is close to the maximum of the Hartley absorption band of ozone [2, 17]. The measurements were instantaneous and did not suffer from errors that may arise due to the presence of nitrogen oxides in the gas [2]. The output gas from the ozonizer was exhausted to the atmosphere via a charcoal (activated carbon) trap (Figure 1).

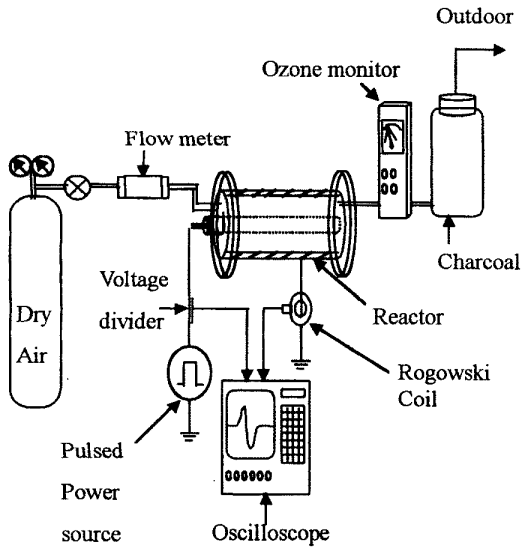

Figure 1. Experimental setup for generation of ozone.

A HV pulse was applied to the central electrode and was obtained from a magnetic pulse compressor (MPC), which can be operated at a variable pulse rate to 500 pulses per second (pps) and to 62 kV peak voltage. A brief description and a circuit diagram of the MPC recently have been given, and further details may be found therein [13]. A positive polarity pulse was applied to the central electrode because with this polarity the production of ozone was higher than with the negative polarity [18, 19]. The positive streamers in the wire-plane geometry in air had substantially more streamers and more branching per unit length of the wire than for negative streamers [11]. The positive streamer extended through the whole gap, while the negative streamer was confined to a smaller region in the vicinity of the wire [19].

The duration of the pulse with ceramic dielectric was typically 100 ns, which was measured at 31 kV, pulse repetition rate of 100 pps, 1.5 l/min dry air flow rate, 15 mm gap length and 157 mm reactor length. The duration of the pulse is defined as the full-width half maximum (FWHM) of the positive pulsed voltage. The output voltage and the discharge current were determined using a combination of a HV capacitive divider, a Rogowski coil and a calibrated Hewlett Packard digital oscilloscope (HP54542A). The latter had a maximum bandwidth of 500 MHz and a maximum sample rate of 2×10^9 s^{-1}.

The energy input to the discharge per pulse is $\int vidt$, where v is the voltage (in V), i the discharge current (in A) and t the time (in s), and was determined from the digitized signals using a computer. The production yield η of ozone in mol/kWh was determined from

$$\eta = \frac{3.6FN}{22.4\times60fE} \quad (1)$$

where F is the gas flow rate in the discharge reactor (in l/min), N the concentration of ozone (in ppm), f the pulse repetition rate (pulses/s) and E the input energy to the reactor per pulse (J/pulse). Since 48 g of ozone is equivalent to 1 mol, and 22.4 l at 1.01×10^5 Pa and 273 K, Equation (1) may be used to give the yield in g/kWh by multiplying it by 48.

2.2 DISCHARGE REACTOR CONFIGURATIONS

Figure 2 shows the electrodes and solid dielectric configurations of three reactors used to produce ozone. Two types of reactors without (Type I) and with (Type II) a solid dielectric layer were employed. All reactors employed coaxial concentric cylindrical electrodes. In both types the central electrode consisted of a spiral wire of 1 mm in diameter wound in either 5 or 10 mm pitch on a PVC tube, either 22 or 26 mm in outer diameter. In Type I, the coiled wire on the PVC tube (10 mm pitch) was placed concentric in a copper cylinder having an inner diameter of 58 mm, which formed the cathode. In Type I, the gaseous gap distance between the wire and the outer cylinder was fixed at 15 mm. Several reactor lengths were employed. A short length of 0.157 m was used for comparison of the performance of three reactors of Type I, Type IIC and Type IIPa and a long one of 1 m for comparison of Type I with Type IIPa (Figure 2). The gap distance between electrodes of all the reactors (1 to 5) used for comparison was kept constant at 15 mm.

The second type (Type II) of discharge reactors contained a dielectric layer made of either a ceramic tube (Type IIC) (outer diameter, 58 mm; ceramic layer thickness, 6 mm; length, 157 mm) or a PVC tube (Type IIP) (outer diameter, 58 or 38 mm; PVC layer thickness, 4 or 3.5 mm; lengths, 0.1 to 1 m) as a dielectric layer. Three different reactors of Type IIP were employed, the details of which are given in Figure 2. The dielectric layer which acts as a barrier to the onset of the breakdown was wrapped on its outside with a copper foil 0.1 mm thick. The copper foil formed the cathode.

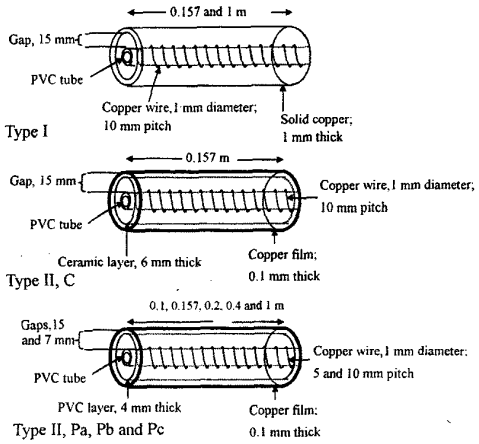

Figure 2. Reactor configurations without (Type I) and with (Type IIC and P) dielectric layers.

Table 1. Details of the ten discharge reactors employed. In all cases anode copper wire, 1 mm in diameter wound with pitch length w_l on a PVC tube, t_d outer diameter. The cathode inner diameter is c_d, the reactor length r_l. g_g gaseous gap, g_e electrode gap. The dielectric outer diameter d_o, inner diameter d_i, and thickness d_t. All dimensions in mm.

No.	Type	g_g	g_e	Diel.	d_o	d_i	d_t	w_l	t_d	c_d	r_l
1	I	15	15	–	–	–	–	10	26	58	157
2	I	15	15	–	–	–	–	10	26	58	1000
3	IIC	9	15	Ceramic	58	46	6	10	26	58	157
4	IIPa	11	15	PVC	58	50	4	10	26	58	157
5	IIPa	11	15	PVC	58	50	4	10	26	58	1000
6	IIPb	3.5	7	PVC	38	31	3.5	10	22	38	100
7	IIPb	3.5	7	PVC	38	31	3.5	10	22	38	200
8	IIPb	3.5	7	PVC	38	31	3.5	10	22	38	400
9	IIPc	3.5	7	PVC	38	31	3.5	5	22	38	200
10	IIPc	3.5	7	PVC	38	31	3.5	10	22	38	200

For the study of the dependence of ozone concentration on the length of the reactor, Type IIPb and Type IIPc reactors (Table 1) were used with 3.5 mm gaseous gap length between the wire and the PVC dielectric layer. For the dependence of the performance of the ozonizer on its length, the length of the reactor (Type IIPb) was varied from 0.1 to 0.4 m and two different flow rates of 1.5 and 3.0 l/min were used. For the study of the dependence of the ozonizer performance on the wire pitch in the anode, reactor Type IIPc was used with a fixed reactor length (0.20 m) and flow rates of 1.5 and 3.0 l/min. The gas pressure was fixed at 1.01×10^5 Pa and the temperature was at 26±4°C throughout this work. Details of the ten discharge reactors employed are given in Table 1.

3 RESULTS AND DISCUSSION

A typical pulsed voltage applied to the discharge reactor Type IIC and the resultant current is shown in Figure 3. The peak voltage was determined at the maximum positive value of the wave including the oscillations. The latter arose from the capacitance of the capacitive divider in combination with the circuit inductances. The oscillations at the peak of the pulsed voltage were generally <3% of the peak voltage. More details including the oscillations at the tail of the voltage wave, which arose from reflections due to impedance mismatch between the power source and the discharge reactors, were discussed recently [20] and they are omitted here for brevity. The duration of the pulse was determined from the FWHM of the positive voltage, typically 110 ns (Figure 3).

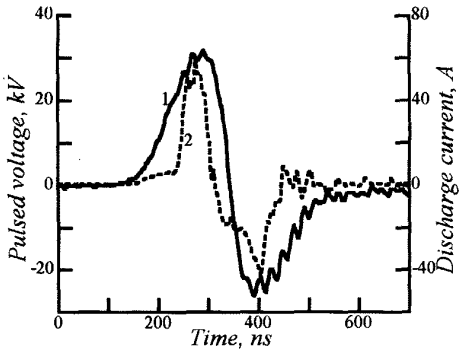

Figure 3. Typical pulsed voltage (1) and discharge current (2) waveforms produced by a MPC in a dielectric barrier discharge of Type IIC reactor (reactor #3). Conditions: gas, dry air; flow rate, 1.5 l/min; pulse repetition rate, 100 pps; details of the reactor as in Table 1 and Figure 2.

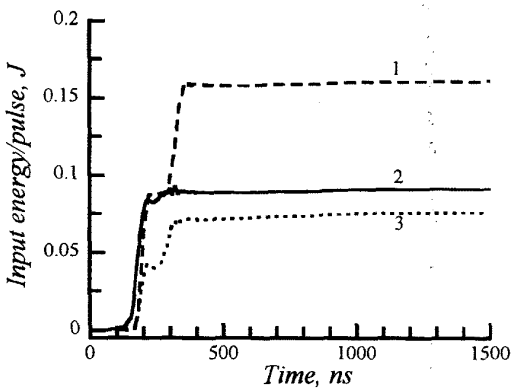

Figure 4. Typical input energy plots to the discharge as a function of time. Conditions: peak pulsed voltage, 30 kV; type of reactors: curve 1, Type IIC (reactor #3); curve 2, Type I (reactor #1); curve 3, Type IIPa (reactor #4); gas, dry air; flow rate, 3 l/min; gas pressure, 1.01×10^5 Pa; gas temperature, 26±4°C; pulse repetition rate, 100 pps; details of the reactors as in Figure 2 and Table 1.

Typical input energy as a function of time of the pulse into different discharge reactors per pulse for a fixed peak applied voltage of 30 kV is shown in Figure 4. It will be observed that the total energy that can be coupled into the discharge strongly depends on the reactor type. This is because the resulting discharge current depends on the length of the gaseous gap, which was different for the three types of reactors (Table 1) although the gap length between the electrodes was constant. In all cases the energy reached a steady state value after ~ 350 ns.

The discharge reactor incorporating a ceramic barrier had the highest energy that can be coupled into it (Figure 4). It will be shown later that this property generally leads to higher ozone concentrations.

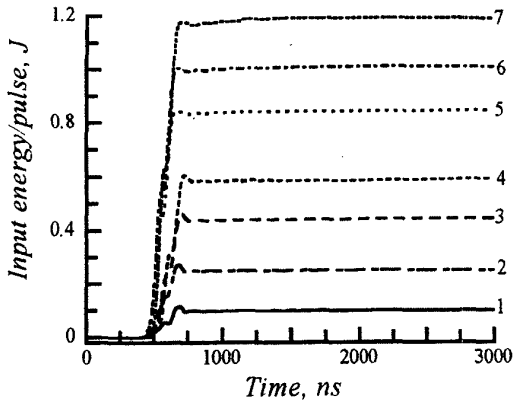

Figure 5. Typical input energy plots of Type IIPa reactor (reactor #5) to the discharge as a function of time for different peak pulsed voltages. Conditions: gas, dry air; pressure, 1.01×10^5 Pa; temperature, 26±4°C; pulse repetition rate, 100 pps; flow rate, 3 l/min; details of the reactor as in Table 1 and Figure 2; peak pulsed voltages and peak currents: curve 1, 26.9 kV, 33.5 A; curve 2, 31 kV, 80.5 A; curve 3, 36.6 kV, 103 A; curve 4, 42.8 kV, 173 A; curve 5, 47.1 kV, 213.2 A; curve 6, 49.5 kV, 200 A; curve 7, 51.3 kV, 219.5 A.

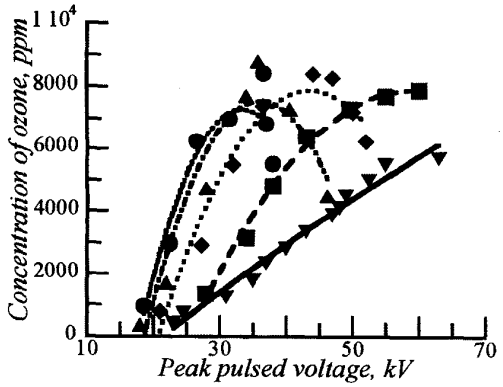

Figure 6. Dependence of the concentration of ozone on pulse voltage of Type IIPa reactor (reactor #5). Conditions: gas, dry air; pressure, 1.01×10^5 Pa; gas temperature, 26±4°C; flow rate, 3.0 l/min; details of the reactor as in Table 1 and Figure 2; pulse repetition rates: ▼ 25 pps; ■ 50 pps; ♦ 100 pps; ▲ 200 pps; ● 400 pps.

Figure 5 shows the energy input per pulse as a function of time for different peak voltages into a specific reactor (Type IIPa, reactor #5). It will be observed that the energy that was coupled into the discharge increased with increasing voltage, but the increase is much larger at higher voltage. For example, when the applied voltage increased from 26.9 to 51.3 kV (1.91×), the energy per pulse increased from 0.10 to 1.19 J (11.9×). This is because the discharge current increased much more than linearly with increasing voltage from 33.5 A at 26.9 kV to 219.5 A (6.6×)

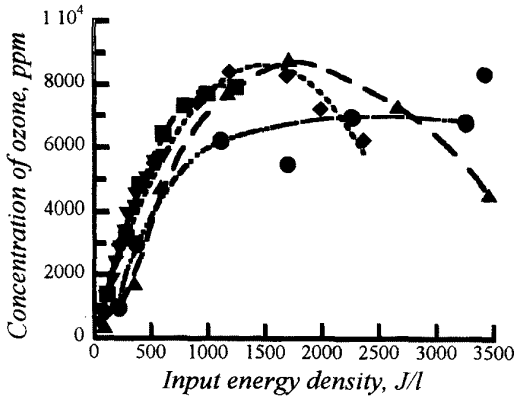

Figure 7. Dependence of the concentration of ozone in Type IIPa reactor (reactor #5) on the energy density input into the discharge. Symbols and conditions as in Figure 6.

at 51.3 kV. This was due to the nonlinear increase in the conductivity of the discharge at HV arising from the increased ionization and electron mobility at the higher electric fields.

3.1 CONCENTRATION OF OZONE

Figure 6 shows the concentration of ozone as a function of the peak pulsed voltage in reactor (Type IIPa, reactor #5) for different pulse repetition rates. It will be observed that the concentration of ozone at low repetition rates ($\leq$ 50 pps) increased steadily with increasing peak voltage to 62 kV, the maximum voltage available from the MPC source. At higher repetition rates, the ozone concentration increased with increasing voltage, reached a maximum and then started to decrease with a further increase in the voltage. The onset of the decrease in the ozone concentration occurred at high concentrations of $\sim$ 7000 ppm and using pulse rates >50 pps, with further increasing voltage (Figure 6). It should be noted that this phenomenon was not observed in pure O_2 [20] or in air using a discharge reactor without a dielectric barrier [13]. However, in the latter study, the peak voltage was limited to much lower values due to the onset of complete breakdown of the gap and the ozone concentration was limited to <5000 ppm for pulse rates $\leq$ 50 pps. The maximum voltage that could be applied to the reactor with the PVC barrier was limited by MPC and not by arc breakdown. A possible reason for the reduction of ozone concentration at higher voltages is that at high concentration of ozone in air, several reactions become possible leading to some losses in the ozone concentration as observed in Figure 6. The following reactions involving the loss of ozone have been reported to occur in air [21]

$$N_2 + O_3 \rightarrow N_2 + O_2 + O \qquad k_2 = 2\times10^{-26}\ cm^3/s \quad (2)$$

$$O + O_3 \rightarrow 2O_2 \qquad k_3 = 1\times10^{-14}\ cm^3/s \quad (3)$$

$$NO_2 + O_3 \rightarrow NO_3 + O_2 \qquad k_4 = 3\times10^{-17}\ cm^3/s \quad (4)$$

$$NO + O_3 \rightarrow NO_2 + O_2 \qquad k_5 = 1.8\times10^{-14}\ cm^3/s \quad (5)$$

$$N + O_3 \rightarrow NO + O_2 \qquad k_6 = 1\times10^{-16}\ cm^3/s \quad (6)$$

$$O(^1D) + O_3 \rightarrow 2O + O_2, \qquad k_7 = 1.2\times10^{-10}\ cm^3/s \quad (7)$$

$$O(^1D) + O_3 \rightarrow 2O_2 \qquad k_8 = 1.2\times10^{-10}\ cm^3/s \quad (8)$$

Ozone may be decomposed also by electron impact [22]

$$e + O_3 \rightarrow e + O_2 + O \quad (9)$$

The reaction rate for (9) has not been measured [22]. Reaction (3) has also been suggested in [1, 23–26] and reaction (5) in [23, 24]. Reaction (5), which involves NO has a larger rate in reducing O_3 than reaction (4). NO is formed in air from the following [21] reactions

$$N + O + N_2 \rightarrow NO + N_2 \qquad k_{10} = 1.0\times10^{-32}\ cm^6/s \quad (10)$$

$$N + O_2 \rightarrow NO + O \qquad k_{11} = 1.0\times10^{-16}\ cm^3/s \quad (11)$$

The dependence of the ozone concentration on the input energy density into the discharge is shown in Figure 7. It will be seen that the ozone concentration increased steadily with increasing input energy density to ~ 1700 J/l, and then saturation was reached, followed by a reduction in the concentration. Increasing the energy input into the discharge above this level for <400 pps is counter productive, because the destruction reactions of ozone exceed its formation. For 400 pps, a saturation in the concentration was reached at ~ 1000 J/l.

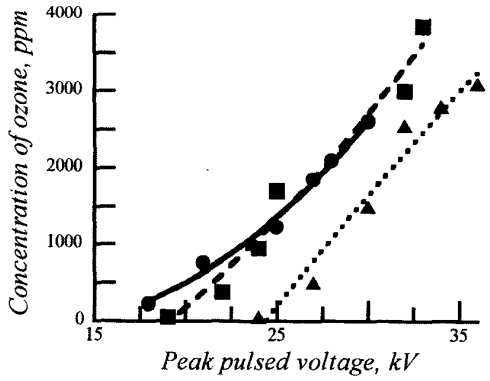

Figure 8. Dependence of concentration of ozone on peak pulsed voltage for three types of reactors. Conditions: gas, dry air; pressure, 1.01×10^5 Pa; gas temperature, 26±4°C; flow rate, 1.5 l/min; pulse repetition rate, 100 pps; Type of reactor, ● Type I (reactor #1), ■ Type IIC (reactor #3); ▲ Type IIPa (reactor #4); details of the reactors as in Table 1 and Figure 2.

A comparison of the production of ozone and the discharge current on peak pulsed voltage, input energy density and peak discharge current, for three different reactors are presented in Figures 8 to 11. It will be observed that the discharge reactor with the PVC barrier gave the lowest ozone concentration, while the ceramic barrier gave the highest concentration for a fixed applied peak voltage (Figure 8) and a fixed discharge current (Figure 10). Further, at a fixed input energy density

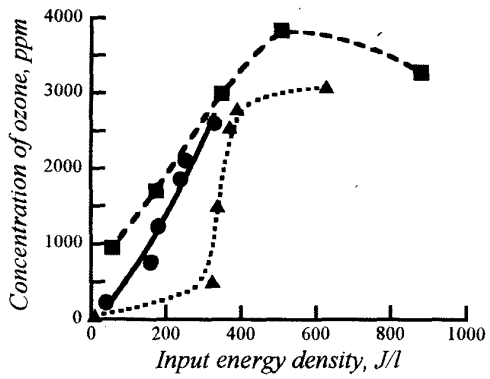

Figure 9. Dependence of concentration of ozone on input energy density for three different types of reactors. Symbols and conditions as in Figure 8.

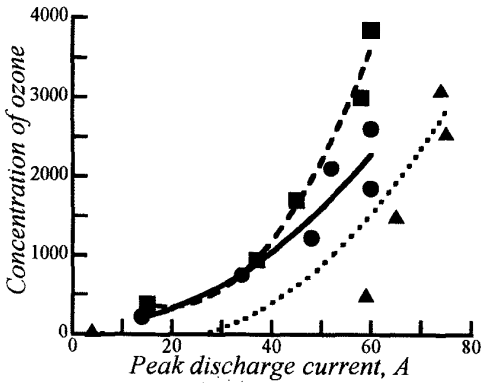

Figure 10. Dependence of concentration of ozone on peak discharge current for three different types of reactors. Symbols and conditions as in Figure 8.

into the three reactors, the highest concentration of ozone was obtained with Type IIC containing the ceramic barrier (Figure 9). The reasons for these findings are attributed to the higher field in the gaseous gap of Type IIC (reactor #3) compared to Type IIPa (reactor #4) at a fixed applied voltage. This was because of the higher permittivity of ceramic alumina (5.6 at 1 MHz and room temperature [15]) compared to the PVC (3.3 at 1 MHz and 25°C [15]). Further reasons are its shorter gaseous gap (9 mm in Type IIC reactor #3) compared to 11 mm in Type IIPa (reactor #4)). The higher electric field in the gaseous gap at a fixed peak voltage in Type IIC resulted in the production of higher energy electrons leading to a higher production of the O radical and therefore, a higher production of O_3 as observed in Figures 8 and 9. The reason for the higher concentration of ozone in the Type I (reactor #1) than in Type IIPa (reactor #4) (Figure 8) is that the temperature of the reactor containing a PVC dielectric barrier was slightly higher than that in the reactor without a dielectric barrier. It has been reported that a slight increase in the gas temperature of ~ 10°C led to substantial reduction in the production of ozone of a factor of ~ 2 in air [27]. In pure oxygen, the ozone production also decreased from 220 to 170 g/m^3 with increas-

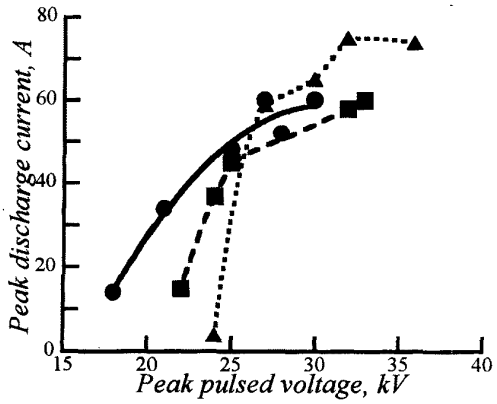

Figure 11. Dependence of peak discharge current on pulsed voltage for three different types of reactors. Symbols and conditions as in Figure 8.

ing temperature of the cooling water of the reactor from 5 to 35°C [31]. Figure 11 shows that the peak of the discharge current increases with increasing peak voltage until saturation is reached at >30 kV for all three reactor types. At a fixed peak voltage of <26.9 kV, the discharge current was higher for the reactor without a dielectric barrier (Figure 11).

3.2 DEPENDENCE OF OZONE PRODUCTION ON REACTOR LENGTH

The dependence of the concentration of ozone on the length of the reactor using Type IIPb is shown in Figures 12 and 13 for 1.5 and 3.0 l/min flow rates, respectively. It will be observed that at fixed applied peak pulsed voltage, the concentration of ozone increased with increasing length of the reactor and decreased with increasing gas flow rate (Figures 12 and 13). This is attributed to the longer residence time of the gas with increasing length of the reactor and decreasing gas flow rate. Typically, the residence time for 1.5 l/min flow rate increased from 2.73 s (reactor #6) to 5.45 s (reactor #7) and to 10.9 s (reactor #8), respectively with increasing length of the reactor, from 0.1 to 0.2 and to 0.4 m. For 3.0 l/min the residence time increased from 1.36 s to 2.73 s and to 5.45 s with increasing reactor length, respectively from 0.1 to 0.2 and to 0.4 m. The longer residence time of the gas in the reactor, the higher would be the production of ozone because of the increased dissociation of O_2 into radicals. This is due to the increased number of collisions with electrons with increasing time, followed by increased collisions of the radicals with O_2 to form O_3. The corresponding energy density input is shown in Figures 14 and 15, respectively for 1.5 and 3.0 l/min flow rates. Figures 14 and 15 show that the ozone productions at a fixed energy density input into the discharge increased with increasing length of the reactor, using the same reactor type, due to the increased residence time of the gas. This is consistent with previously reported results, which showed that for short residence time (<5 s) the concentration of O_3 increased with increasing residence time [27].

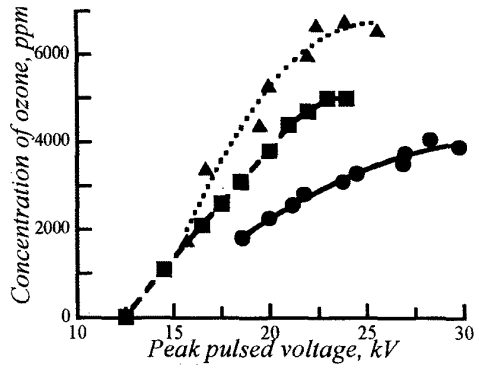

Figure 12. Dependence of the concentration of ozone using Type IIPb reactors on applied peak pulsed voltage for different reactor lengths for 1.5 l/min flow rate. Conditions: gas, dry air; pressure, 1.01×10^5 Pa; temperature, 26±4°C; pulse repetition rate, 100 pps; reactor lengths: ● 0.1 m (reactor #6); ■ 0.2 m (reactor #7); ▲ 0.4 m (reactor #8); other details of the reactors as in Table 1 and Figure 2.

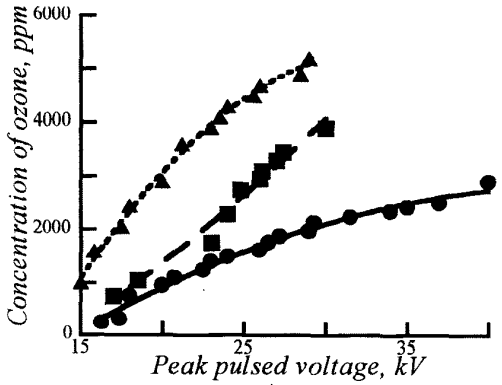

Figure 13. Dependence of the concentration of ozone using Type IIPb reactors on applied peak pulsed voltage for different reactor lengths (reactors #6 to 8) for 3.0 l/min flow rate. Conditions and symbols as in Figure 12.

3.3 DEPENDENCE OF OZONE CONCENTRATION ON PITCH LENGTH

The dependence of the ozone concentration on the pitch length is shown in Figure 16 using reactor Type IIPc (reactors #9 and 10, Table 1). It will be observed that at a fixed applied peak pulsed voltage and a fixed gas flow rate, the longer pitch length of 10 mm of the wire forming the anode (Figure 2) led to a higher ozone concentration than for 5 mm pitch length (Figure 16). This was the case for both flow rates of 1.5 and 3.0 l/min. A very short pitch winding of the wire forms a continuous solid rod with a consequent lower electric field closer to the wire, due to the large diameter of the PVC on which it was wound. Therefore, the longer pitch length, having a wider separation between the turns of the wire resulted in a higher field near the central electrode leading to a higher production of ozone as indeed observed in Figure 16.

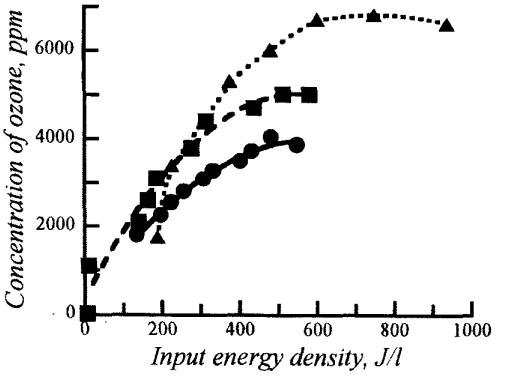

Figure 14. Dependence of the concentration of ozone on input energy density to the discharge for 1.5 l/min flow rate in Type IIPb reactors for different reactor lengths (reactors # 6 to 8). Symbols and other conditions as in Figure 12.

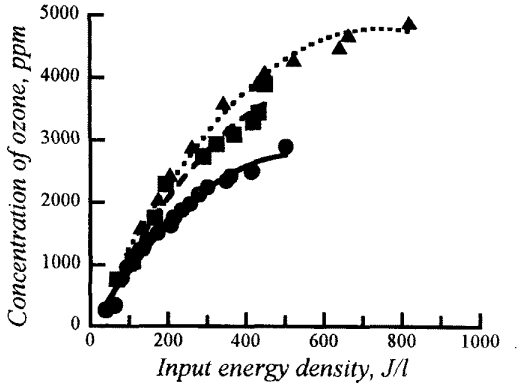

Figure 15. Dependence of the concentration of ozone on energy density input to the discharge for 3.0 l/min flow rate in Type IIPb reactors for different reactor lengths (reactors #6 to 8). Symbols and other conditions as in Figure 12.

Figure 17 shows the dependence of the concentration of ozone on the energy density input into the discharge for different pitch lengths of the anode wire in reactor Type IIPc (reactors #9 and 10). It will be observed from Figure 17 that at a constant energy density input and a constant flow rate of the gas into the reactor, a higher concentration of ozone was obtained. The reason for this is attributed to the presence of a higher electric field near the anode for the longer pitch length, where most of the production of ozone occurs.

3.4 DEPENDENCE OF OZONE CONCENTRATION ON THE FLOW RATE

Figures 16 and 17 show the dependence of the ozone concentration on the flow rate. At a fixed peak pulsed voltage and a fixed pitch length of the wire, the lower flow rate of 1.5 l/min led to a higher production of ozone compared to 3.0 l/min (Figure 16). Similar behavior was observed at a constant energy density input into the discharge (Figure 17).

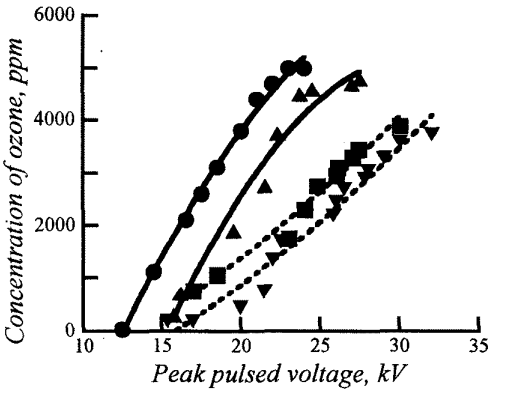

Figure 16. Dependence of the concentration of ozone on peak pulsed voltage for different flow rates and different pitch lengths of the spiral copper wire in reactor Type IIPc (reactors #9 and 10) Conditions: gas, dry air; pressure, 1.01×10^5 Pa; temperature, 26±4°C; pulse repetition rate, 100 pps; flow rates and pitch lengths, ● 1.5 l/min and 10 mm; ■ 3.0 l/min and 10 mm; ▲ 1.5 l/min and 5 mm; ▼ 3.0 l/min and 5 mm; other details of the reactor as in Table 1 and Figure 2.

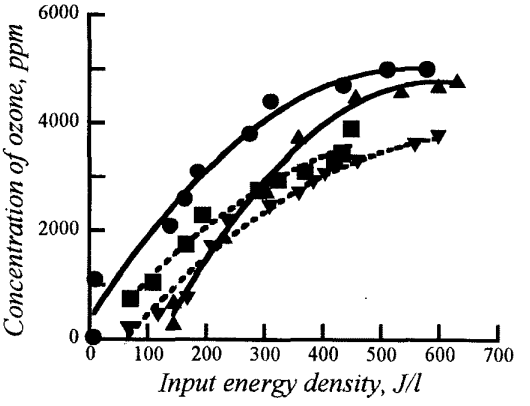

Figure 17. Dependence of the concentration of ozone of Type IIPc reactors (reactors #9 and 10) on energy density input to the discharge. Symbols and conditions as in Figure 16.

The increased production of ozone at lower flow rate is attributed to the increased residence time in the reactor as explained in Section 3.2.

3.5 PRODUCTION YIELD OF OZONE

3.5.1 DEPENDENCE ON THE PEAK PULSED VOLTAGE

Figure 18 shows the production of ozone in 1 m long reactor of Type IIPa (reactor #5) *vs.* peak pulsed voltage for different pulse rates. It will be seen that the production yield initially increased with increasing voltage ($\leqslant$ 30 kV) for pulse rates $\leqslant$ 100 pps and then decreased with further increase in the applied pulsed voltage. The initial increase in the yield with increasing voltage is attributed to the increased concentration of O_3 with increasing voltage (<30 kV) (Figure 6) while the energy input to the discharge increased linearly with voltage (Figure 19). The

decrease in the yield at >30 kV (Figure 18) is attributed to the reduction of the concentration of O_3 with increasing voltage (Figure 6) and the larger than linear increase of the energy input into the discharge at higher voltages (Figure 19). The larger increase in the energy input to the discharge was due to the much higher discharge currents with increased voltages (see caption of Figure 5) arising from higher ionization and larger electron velocities at higher voltages leading to increased conductivity of the plasma. Figure 18 also shows that at a fixed pulsed voltage (>30 kV), the production yield decreased with increasing pulse rate. Typically at 37 kV, the yield decreased in this reactor from 89.1 g/kWh at 25 pps to 14.9 g/kWh at 400 pps (Figure 18); this is generally consistent with Equation (1). In the low voltage region (<30 kV) the highest yield was achieved in this reactor at 100 pps of ~ 94.9 g/kWh at 27 kV applied peak pulsed voltage (Figure 18). It should be noted that it was not possible to attain maxima values of the concentration and of the yield of ozone simultaneously using the same operating conditions.

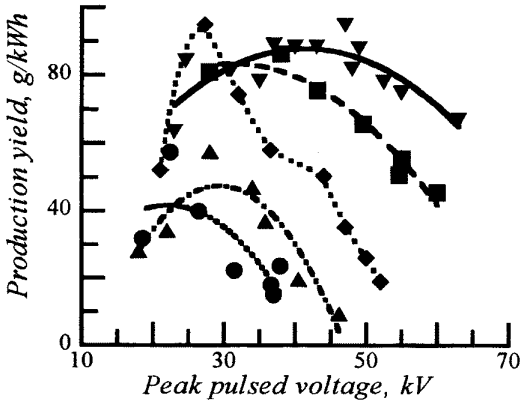

Figure 18. Dependence of the production yield of ozone on peak pulsed voltage for different pulse rates in Type IIPa reactor (reactor #5). Conditions: gas, dry air; pressure, 1.01× 105 Pa; gas temperature, 26±4℃; flow rate, 3.0 l/min; details of the reactor as in Table 1 and Figure 2; pulse repetition rates: ▼ 25 pps; ■ 50 pps; ♦ 100 pps; ▲ 200 pps; ● 400 pps.

Figure 20 shows a comparison of the production yield of ozone for three types of reactors (#1, 3 and 4) while maintaining the same conditions of flow rate (1.5 l/min), reactor length (157 mm), electrode gap separation (15 mm) and pulse rate (100 pps). It will be observed that Type IIC reactor with the ceramic layer produced the highest yield of 122 g/kWh at 24 kV peak pulsed voltage. This is attributed to the higher production of O_3 in the Type IIC reactor at a fixed peak pulsed voltage (Figure 8) and a fixed energy density input (Figure 9) as shown in Section 3.1. The maxima of the production rate for reactors Type IIPa (with PVC dielectric layer) and Type I (without a dielectric layer) were 52 and 60 g/kWh (Figure 20). The production yield of O_3 in the three reactors was strongly dependent on the peak pulsed voltage (Figure 20). This is because the concentration of O_3 (Figures 6, 8, 12, 13 and 16) and the energy input into the discharge (Figure 19) varied with the applied voltage. Figure 21 shows the production rate of O_3 against peak pulsed voltage for two types of reactors of 1 m in length. It will be

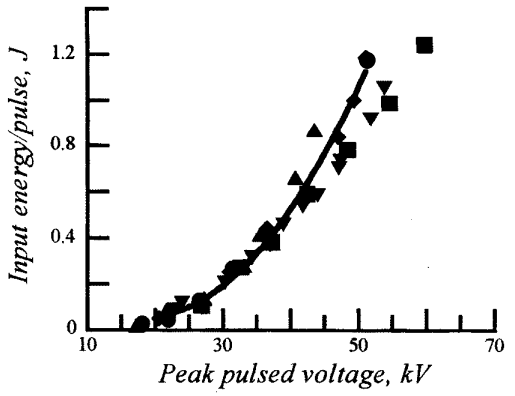

Figure 19. Dependence of the input energy to the discharge per pulse on the applied peak pulsed voltage in reactor Type IIPa (reactor #5). Flow rate, 3.0 l/min; other conditions and symbols as in Figures 6 and 18.

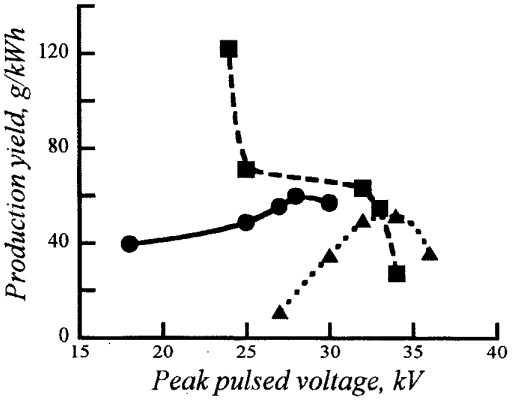

Figure 20. Dependence of the production yield of ozone on peak pulsed voltage for three different reactors 157 mm long (reactors #1, 3 and 4). Conditions: gas, dry air; pressure, 1.01×10^5 Pa; gas temperature, 26±℃;4 flow rate, 1.5 l/min; pulse repetition rate, 100 pps; Type of reactor; ● Type I (reactor #1), ■ Type IIC (reactor #3); ▲ Type IIPa (reactor #4).

observed that Type I (reactor #2) had a slightly higher production yield than the reactor containing a PVC dielectric barrier (reactor #5), which was consistent with the results obtained when a shorter length reactors of 157 mm were employed (Figure 20). The higher value of the production yield in Type I was due to larger production of O_3 (see Figure 8 for 157 mm long reactors; for 1 m long reactors figure is omitted for brevity). The energy input into the discharge for the two reactors and for peak pulsed voltages $\leqslant$27 kV were close (figure omitted for brevity).

3.5.2 DEPENDENCE OF PRODUCTION YIELD ON LENGTH OF THE REACTOR

Figure 22 shows the production yield of O_3 for different lengths of discharge reactors using Type IIPb (reactors #6 to 8). The dependence of

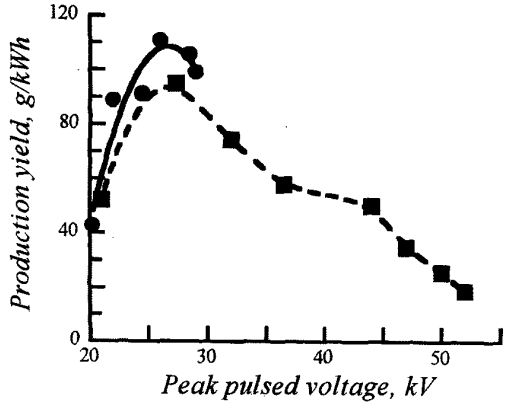

Figure 21. Dependence of the production yield of ozone on peak pulsed voltage for 1 m long reactors. Conditions: Flow rate, 3 l/min; pulse rate, 100 pps; type of reactor, ● Type I (reactor #2), ■ Type IIPa (reactor #5).

the production yield is related to the dependence of the concentration (Figure 12) and the energy input (Figure 23) of the discharge on the applied peak pulsed voltage. It will be observed from Figure 23 that at a fixed applied voltage, the energy input into the discharge increased with increasing length of the reactor. This is because at a fixed applied voltage, the discharge current increased with increasing length of the reactor. The current increased due to the increased conductivity of the plasma discharge with increasing number of streamers in the longer reactors. Figure 22 shows that for 1.5 l/min, the highest yields of 122, 105 and 96 g/kWh were obtained, respectively for 0.2, 0.4 and 0.1 m long reactors.

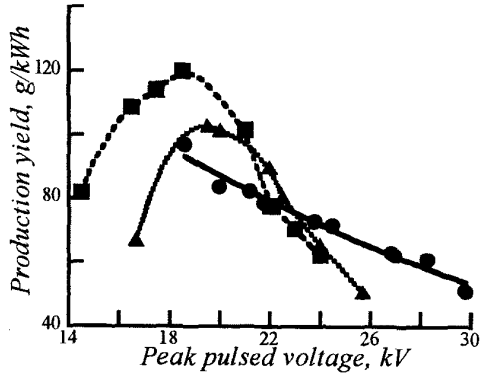

Figure 22. Dependence of the production yield of ozone on peak pulsed voltage in Type IIPb for different lengths of reactors. Conditions: flow rate, 1.5 l/min; pulse rate, 100 pps; reactor lengths, ● 0.1 m (reactor #6), ■ 0.2 m (reactor #7), ▲ 0.4 m (reactor #8).

3.5.3 DEPENDENCE OF PRODUCTION YIELD ON OZONE CONCENTRATION

Figure 24 shows the production yield *vs.* ozone concentrations for the three types of reactors. The reactor with ceramic (reactor #3) had

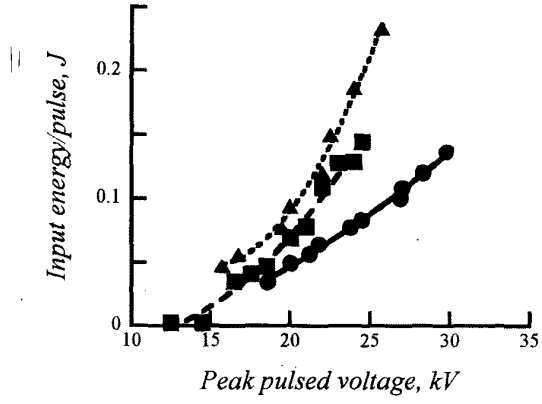

Figure 23. Dependence of the input energy to the discharge per pulse on the applied peak pulsed voltage for different lengths of reactor Type IIPb. Symbols and conditions as in Figure 22.

the highest yield over a wide range of ozone concentration and it decreased with increasing concentration. For reactors Type I (reactor #1) and Type IIPa (reactor #4) the production yield increased with increasing concentration but the yield values were smaller than for Type IIC. Figure 25 shows the production yield of O_3 *vs.* its concentration for different lengths of reactor Type IIPb. It will be observed that the production yield at a fixed concentration is higher for the longer reactor.

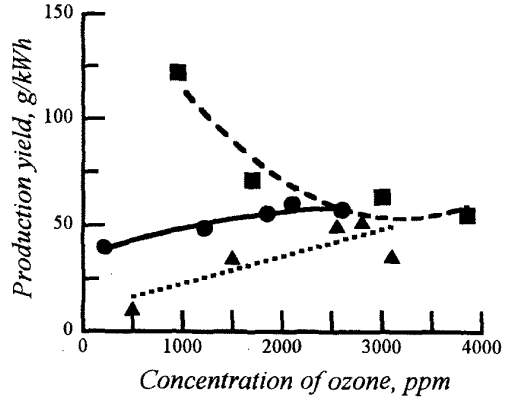

Figure 24. Production yield of ozone *vs.* its concentration for three types of reactors. Conditions: flow rate, 1.5 l/min; reactor length, 157 mm; pulse rate, 100 pps; type of reactor, ● Type I (reactor #1), ■ Type IIC (reactor #3), ▲ Type IIPa (reactor #4).

Initially the production yield increased with increasing ozone concentration and then decreased after reaching a maximum. This is because, as shown in Figure 13, the increase in the concentration with increasing voltage becomes less than linear at HV. Therefore, the input energy is also increased at a higher rate than the concentration of ozone, leading to a reduced yield at higher voltages and therefore at higher concentrations (Figure 25).

Figure 26 shows the production yield for different pitch lengths of the anode wire in reactor Type IIPc (reactors #9 and 10) as a function

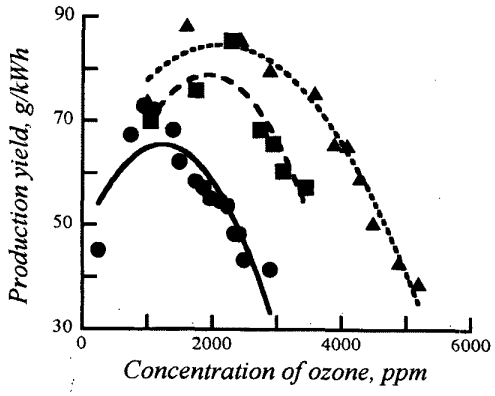

Figure 25. Production yield of ozone *vs.* its concentration for different lengths of the reactor Type IIPb. Conditions: flow rate, 3 l/min; pulse rate, 100 pps; reactor lengths, ● 0.1 m (reactor #6), ■ 0.2 m (reactor #7), ▲ Type IIPa (reactor #8).

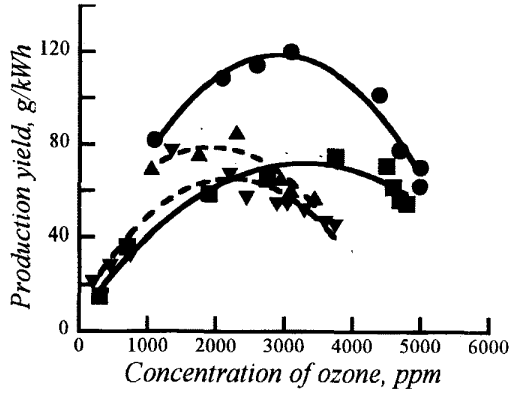

Figure 26. Production yield of ozone *vs.* its concentration for different pitch length of the anode wire and different flow rates using reactor Type IIPc. Flow rates and pitch lengths: ● 1.5 l/min and 10 mm (reactor #10); ■ 3.0 l/min and 10 mm (reactor #10); ▲ 1.5 l/min and 5 mm (reactor #9); ▼ 3.0 l/min and 5 mm (reactor #9).

of the ozone concentration. It will be observed that the higher yield of 122 g/kWh was obtained for the longer pitch length of 10 mm and the lowest flow rate of 1.5 l/min (reactor #10). This is attributed to the longer residence time at the lower flow rate and the higher field at a longer pitch length, which led to a higher production of ozone (Figure 16) and therefore a higher yield.

3.5.4 COMPARISON OF PRODUCTION YIELD WITH OTHER WORKS

In commercial systems the production yield of ozone in air was reported to be 50 to 55.6 g/kWh (18 to 20 kWh/kg) [28]. Masuda *et al.* [19] reported values in dry air using a dielectric barrier with strip plates from 77.4 to 200 g/kWh. Pietsch *et al.* [29] reported a yield of 27.07 g/kWh in air using a dielectric barrier discharge. Chalmers *et al.* using a pulsed voltage of 120 ns width, reported a yield of 147 g/kWh in O_2 without a dielectric barrier [7, 30]. Our results compare very favorably with the previously reported values of the production yield of ozone in dry air.

4 CONCLUSIONS

1. The current and the input energy into the discharge increased nonlinearly with increasing applied pulsed voltage.
2. The concentration of ozone initially increased linearly with increasing applied pulsed voltage, reached a saturation and then declined with further increasing voltage for pulse rate $\geqslant$ 50 pps.
3. The concentration of ozone initially increased with increasing input energy density, reached saturation and then declined with further increase in the input energy density.
4. The concentrations of ozone in the discharge barrier reactors with ceramic were higher than with PVC for the same reactor length and electrode gap distance.
5. The concentration of ozone at a fixed applied pulsed voltage and a fixed input energy density into the reactor increased with increasing reactor length.
6. The concentration of ozone increased with decreasing gas flow rate at a fixed applied pulsed voltage and a fixed input energy density into the discharge.
7. The concentration of ozone increased with increasing the pitch length of the spiral windings of the anode wire.
8. The production yield of ozone (g/kWh) at a fixed applied pulsed voltage decreased with increasing pulse repetition rate.
9. The production yield of ozone initially increased with increasing voltage and then decreased at a fixed pulse repetition rate.
10. The production yield of ozone was higher with a ceramic dielectric barrier discharge than with PVC and without a dielectric layer.
11. The input energy to the discharge per pulse increased with increasing reactor length.
12. The production yield of ozone over a wide range of concentrations was higher in the reactor containing a ceramic dielectric barrier than with PVC or without a barrier.

REFERENCES

[1] B. Eliasson and U. Kogelschatz, "Nonequilibrium Volume Plasma Chemical Processing", IEEE Trans. on Plasma Sci., Vol. 19, No. 6, pp. 1063–1077, 1991.

[2] U. Kogelschatz, "Advanced Ozone Generation", in *Process Technologies for Water Treatment*, S. Stucki, Ed. New York & London: Plenum, pp. 87–120, 1988.

[3] U. Kogelschatz, B. Eliasson and M. Hirth, "Ozone Generation From Oxygen and air: Discharge Physics and Reaction Mechanisms", Ozone Science and Engineering, Vol. 9, pp. 367–377, 1987.

[4] I. Munemiya, Ed., *New Technologies Using Ozone*, Sanshu Press, Yokohama, Mineoka 2-201, 1993 (in Japanese)

[5] B. M. Penetrante and S. E. Schultheis, "Non-Thermal Plasma Techniques for Pollution Control", Springer-Verlag, Series G: Ecological Sciences, Vol. 34, Parts A and B, 1993.

[6] Y. L. M. Creyghton, E. M. van Veldhuizen and W. R. Rutgers, "Electrical and Optical Study of Pulsed Positive Corona", in *Non-Thermal Plasma Techniques for Pollution Control*, Eds. B. M. Penetrante and S. E. Schultheis, Part A, Springer-Verlag, pp. 205–230, 1993.

[7] I. Chalmers, L. Zanella and S. J. MacGregor, "Ozone Synthesis in Oxygen in a Dielectric Barrier Free Configuration", 10th IEEE International Pulsed Power Conference, Albuquerque, pp. 1249–1254, 1995.

[8] A. Mizuno and Y. Kamase, "Emission of Current in Pulsed Streamer Corona Discharge", Conf. Record of IEEE Indust. Appl. Soc. Annual Meeting (Cat. No. 87 CH 2499-2), Vol. 02, pp. 1534–1538, 1987.

[9] H. Akiyama, "Pollution Control by Pulsed Power", Proceedings of International Power Electronics Conference, Yokohama, pp. 1397–1399, 1995.

[10] F. Hegeler and H. Akiyama, "Spatial and Temporal Distributions of Ozone After a Wire-to-Plate Streamer Discharge", IEEE Trans. on Plasma Sci., Vol. 25, No. 5, pp. 1085–1090, 1997.

[11] F. Hegeler and H. Akiyama, "Ozone Generation by Positive and Negative Wire-to-Plate Streamer Discharges", Japan J. Appl. Phys., Vol. 36, pp. 5335–5339, 1997.

[12] G. E. Vogtlin and B. M. Penetrante, "Pulsed Corona Discharge for Removal of NO_x From Flue Gas, in *Nonthermal Plasma Techniques For Pollution Control*, Part B, B. M. Penetrante and S. E. Schultheis, Eds. NATO ASI Series, Series G: Ecological Sciences, Vol. G: 34, Springer-Verlag, pp. 187–198, 1993.

[13] W. J. M. Samaranayake, Y. Miyahara, T. Namihira, S. Katsuki, T. Sakugawa, R. Hackam and H. Akiyama, "Pulsed streamer discharge characteristics of ozone production in dry air", IEEE Trans. DEI, Vol. 7, pp. 254–260, April 2000.

[14] M. Abdel-Salam, A. Mizuno and K. Shimizu, "Ozone generation as influenced by gas flow in corona reactors", J. Phys. D: Appl. Phys. Vol. 30, pp. 864–870, 1997.

[15] R. C. Weast, M. J. Astle and W. H. Beyer, *'CRC Handbook of Chemistry and Physics*, 65th edition, CRC Press, Inc., Boca Raton, Florida, pp. F-157, 1984–1985.

[16] S. Masuda, E. Kiss, K. Ishida and H. Asai, "Ceramic-based ozonizer for high-speed sterilization", IEEE Transactions on Industry Applications, Vol. 26, No. 1, 1990.

[17] L. T. Molina and M. J. Molina, "Absolute absorption cross sections of ozone in the 185 to 350 nm wavelength range", J. Geophys. Vol. 91, pp. 14. 501–14. 508, 1986.

[18] B. Held, "Corona and Their Applications", 11th International Conference of Gas Discharges and Their Applications, Tokyo, Vol. 2, pp. II-514–526, 1995.

[19] S. Masuda, M. Sato and T. Seki, "High-efficiency ozonizer using traveling wave pulse voltage", IEEE Transactions on industry applications, Vol. IA-22, No. 5, pp. 886–891, 1986.

[20] W. J. M. Samaranayake, Y. Miyahara, T. Namihira, S. Katsuki, R. Hackam and H. Akiyama, "Ozone Production Using Pulsed Dielectric Barrier Discharges in Oxygen", IEEE Trans. DEI, Vol. 7, pp. 849–854, December 2000.

[21] J. J. Lowke and R. Morrow, "Theoretical Analysis of Removal of Oxides of Sulfur and Nitrogen in Pulsed Operation of Electrostatic Precipitators", IEEE Trans. on Plasma Science, Vol. 23, pp. 661–671, 1995.

[22] B. Eliasson, M. Hirth and U. Kogelschatz, "Ozone Synthesis From Oxygen in Dielectric Barrier Discharges", J. Phys. D, Appl. Phys., Vol. 20, pp. 1421–1437, 1987.

[23] B. Eliasson and U. Kogelschatz, "Modeling and Applications of Silent Discharge Plasmas", IEEE Trans. on Plasma Science, Vol. 19, No. 2, pp. 309–323, 1991.

[24] U. Kogelschatz and B. Eliasson, "Ozone generation and applications", *Handbook of Electrostatic Processes*, Marcel Dekker, New York, pp. 581–605, 1995.

[25] L. G. Hogan and D. S. Burch, "A measurement of the rate constant for the reaction $O + O_2 + O_2 \rightarrow O_3 + O_2$", J. Chem. Phys. Vol. 65, pp. 894–900, 1976.

[26] J. A. Dorsey and J. H. Davidson, "Ozone Production in Electrostatic Air Cleaners with Contaminated Electrodes", IEEE Trans. Ind. Appl., Vol. 30, pp. 370–375, 1994.

[27] S. Yagi and M. Tanaka, "Mechanism of Ozone Generation in Air-fed Ozonisers", J. Phys. D: Appl. Phys., Vol. 12, pp. 1509–1520, 1979.

[28] U. Kogelschatz, "Silent discharges and their applications", Proc. 10th Int. Conf. on Gas Discharges & their Applications, Swansea, pp. 972–980, 1992.

[29] G. J. Pietsch and V. Gibalov, "Dielectric barrier discharges and ozone synthesis", Pure & Appl. Chem., Vol. 70, pp. 1169–1174, 1998.

[30] I. D Chalmers., L. Zanella, S. J. MacGregor and J. J. Wheatley, "Pulsed ozone generation in oxygen", ICPIG Conference, New Jersey, USA, pp. 125–126, 1995.

[31] J. Kitayama and M. Kuzumoto, "Theoretical and experimental study on ozone generation characteristics of an oxygen-fed ozone generator in silent discharge", J. Phys. D: Appl. Phys. Vol. 30, pp. 2453–2461, 1997.

---

[1] Was on leave from University of Windsor, Department of Electrical and Computer Engineering, Windsor, Ontario, Canada

Manuscript was received on 22 September 2000, in revised form 7 February 2001.